

Reaction of (1*R*,2*S*,3*S*)-3-Methylcyclohexanediamineplatinum(II) with DNA: Isolation and Characterization of the Platinum–Nucleotide Adducts by Means of HPLC and NMR Spectroscopy

Kenji INAGAKI* and Kimie SAWAKI

Laboratory of Chemistry, Seirei Christopher College of Nursing, 3453, Mikatabara-cho, Hamamatsu 433, Japan.

Received August 29, 1994; accepted October 17, 1994

Reaction products of calf thymus DNA with (1*R*,2*S*,3*S*)-3-methylcyclohexanediamineplatinum (abbreviated as Pt(*RSS*-dach)Cl₂) were investigated by enzymatic degradation of the platinated DNA and subsequent HPLC analysis. Five platinated adducts involving d(GpG), d(ApG) and (dG)₂ residues were identified by HPLC after complete digestion using deoxyribonuclease I, nuclease P1, and alkaline phosphatase. The adducts with d(GpG) and d(ApG) consisted of two geometrical isomers, because Pt(*RSS*-dach)Cl₂ lacks a C₂ symmetry element. The d(GpG) and d(ApG) adducts were intrastrand compounds crosslinked between the N7 atoms of the adjacent purine bases. The two d(GpG) adducts were most abundant and comprised more than 65% of all the platinated adducts. The relative ratio of the two d(GpG) isomers was 3:2 for reaction with DNA, whereas the ratio was 1:1 for reaction with a single stranded oligonucleotide. The detailed structure of the two d(GpG) adducts is also described based on NMR spectroscopic data.

Key words cyclohexanediamine platinum complex; platinum DNA adduct; enzymatic digestion product; cisplatin derivative; NMR

Whether or not the modification of DNA by antitumor platinum compounds is responsible for their observed antitumor activity has not been directly proved. However, it is a fact that DNA is a primary target for these platinum compounds.¹ It has been shown that, *in vivo* and *in vitro*, *cis*-dichlorodiammineplatinum(II) (abbreviated as cisplatin) reacts preferentially with adjacent purine residues on the same strand of the DNA double helix and induces bending of this helix. It is very likely that such a modification plays an important role in inhibiting DNA replication.^{1,2} In a search for the platinum binding sites on DNA, enzymatic digestion of cisplatin-modified DNA showed that *cis*-Pt(NH₃)₂(d(GpG)-N7,N7) was the most prominent adduct followed by *cis*-Pt(NH₃)₂(d(ApG)-N7,N7).^{1–3} Also *cis*-Pt(NH₃)₂(dG)₂ was identified among the enzymatic digestion products. The adduct is thought to originate from an intrastrand crosslinking between two guanine residues, separated by at least one

nucleotide residue, and from an interstrand crosslinking between two guanine residues.^{1,3} No platination was observed at adenine N1, cytosine N3 and thymine N3 on DNA.^{1,3} Cisplatin is a complex possessing a C₂ symmetry element. The cisplatin derivatives which lack a C₂ symmetry element, (*e.g.*, *cis*-PtCl₂(LL') in which L = NH₃ and L' = alkylamine), also yield similar adducts.⁴ However, in this case, two geometrical isomers could be formed in the reaction with GpG, *cis*-Pt(LL')(GpG-N7,N7). One has the L *cis* to the 5'-guanine residue while the other has L' *cis* to it. Dichloro(1*R*,2*S*,3*S*)-3-methylcyclohexanediamineplatinum(II) (abbreviated as Pt(*RSS*-dach)Cl₂) does not possess a C₂ symmetry element as is illustrated in Fig. 1. Therefore, it is possible to obtain the two geometrical isomers by binding of Pt(*RSS*-dach)Cl₂ with GpG, as illustrated in Fig. 2. One of the geometrical isomers has the methyl group *cis* to the 5'-guanine residue. While in the other it is *trans*. To understand platinum–

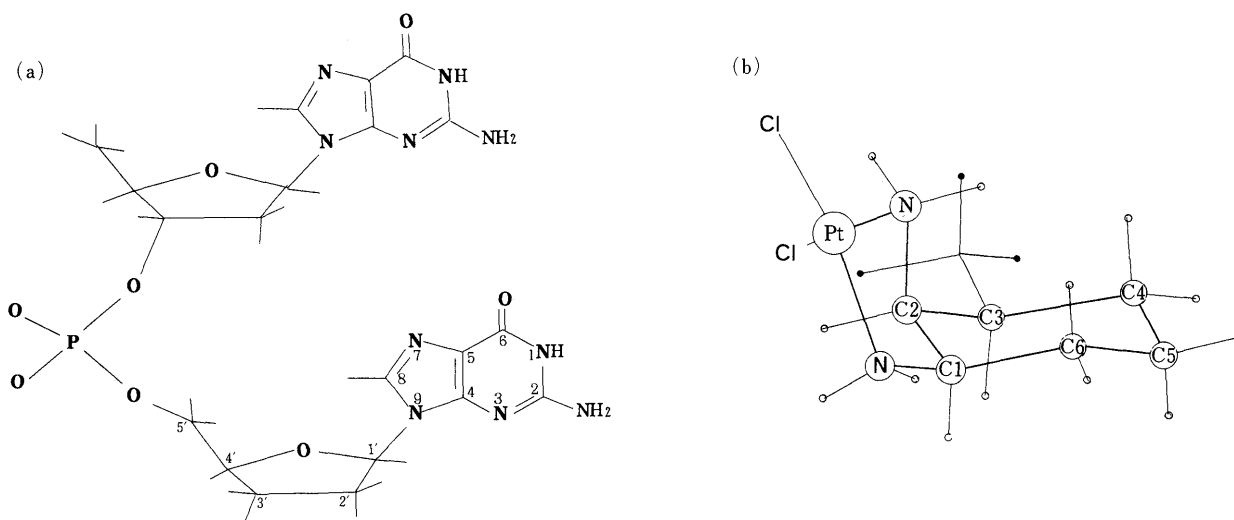


Fig. 1. Schematic Structures and Numbering of d(GpG) and Pt(*RSS*-dach)Cl₂

* To whom correspondence should be addressed.

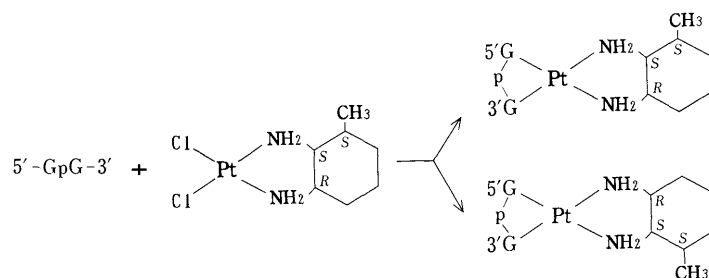


Fig. 2. Possible Orientations of the Two Geometrical Isomers, Pt(*RSS*-dach)(d(GpG))

DNA interactions, it would be useful to investigate whether the asymmetry and stereochemistry of the non-leaving ligand affects the binding to DNA or not. The first part of the present study deals with quantitation of platinum–nucleotide adducts, obtained by the reaction of Pt(*RSS*-dach)Cl₂ with calf thymus DNA. This was carried out by means of enzymatic digestion of the platinated DNA followed by subsequent HPLC analysis. The second part describes the structure of the two geometrical isomers based on an analysis of NMR spectral data.

Experimental

The platinum complex, Pt(*RSS*-dach)Cl₂, was kindly provided by Professor Reiko Saito.⁵⁾ It was dissolved in distilled water and used immediately. Oligonucleotides were synthesized using an Applied Biosystems solid phase synthesizer and purified by reversed phase chromatography on a 5C₁₈ HPLC column. Calf thymus DNA was purchased from Sigma. A stock solution was prepared by dissolving 200 μg/ml DNA in 0.05 M phosphate buffer (pH 7.3) containing 10 mM NaCl. A small aliquot of Pt(*RSS*-dach)Cl₂ aqueous solution was added to the stock DNA solution at concentrations in the range $r = 0.01$ – 0.05 , where r is the molar ratio of platinum per nucleotide. The reaction solutions were incubated in the dark at 37 °C for 24 h and then dialyzed to remove the unreacted platinum complexes. The platinated DNA was digested using deoxyribonuclease I, P1 nuclease and alkaline phosphatase according to the procedures reported previously.³⁾ Firstly, the solution containing the platinated DNA was adjusted to pH 5.5 by adding 0.1 M acetate buffer solution and then treated with deoxyribonuclease I and P1 nuclease at 37 °C for 20 h. This digestion yields mononucleotides and platinated nucleotides. The pH of the solution was then raised to pH 9 by adding 1.0 M Tris–HCl buffer solution followed by treatment with alkaline phosphatase at 37 °C for 4 h in order to remove the terminal 5'-phosphate groups of the digested products. The enzymatic digestion products were separated and identified by HPLC. The HPLC parameters were as follows: column, Cosmosil 5C₁₈, two 4.6 × 250 mm columns joined with a stainless-steel tube; mobile phase, 0.1 M phosphate buffer (pH 3.6) containing 5% acetonitrile; flow rate, 0.8 ml/min; detector, UV at 260 nm. The column temperature was maintained at 27 °C because the separation of the digestion products was significantly affected by temperature.

NMR spectra were recorded at 27 °C on a JEOL JNM-A500 or a JEOL JNM-EX-270 NMR spectrometer. NMR samples were prepared by lyophilizing each sample three times from 99.7% D₂O, and finally dissolving in 99.95% D₂O. The pH of the NMR sample (without correction for the deuterium isotope effect) was between 5 and 6.5, being measured after NMR spectroscopy. The nuclear Overhauser effect (NOE) was measured by the difference spectral mode following careful degassing. For this measurement a pre-irradiation time of 5 s was used for complete saturation. A two-dimensional correlation spectroscopy (COSY) experiment was performed by using the sequence (90°-pulse- t_1 -90°-pulse-acquisition) _{n} , where t_1 = evolution period and n = repeat. NMR spectral simulation was carried out using a LAOCOON-type microcomputer program.⁶⁾

Results and Discussion

In order to explore the reaction products of Pt(*RSS*-

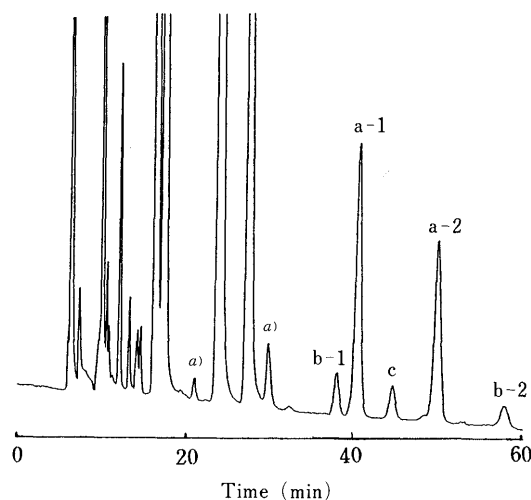


Fig. 3. Chromatogram of the Enzymatic Digestion Products of Pt(*RSS*-dach)-Modified DNA

a-1, Pt(*RSS*-dach)(d(GpG))-1; a-2, Pt(*RSS*-dach)(d(GpG))-2; b-1, Pt(*RSS*-dach)(d(ApG))-1; b-2, Pt(*RSS*-dach)(d(ApG))-2; c, Pt(*RSS*-dach)(dG)₂. a) unidentified peaks.

dach)Cl₂ with DNA, an enzymatic degradation of the platinated DNA was carried out using deoxyribonuclease I, P1 nuclease and alkaline phosphatase.^{3d,4c)} Figure 3 shows a typical chromatogram of the enzymatic digestion products of the platinated DNA. The peaks marked with signs are assigned to the reaction products, *i.e.*, no such peaks were observed in the chromatogram of the digested sample of unplatinated DNA. To confirm the completeness of enzymatic digestion, the same sample was also degraded by other enzymes (deoxyribonuclease I, snake venom phosphodiesterase, alkaline phosphatase, and calf spleen phosphodiesterase).⁷⁾ The result was almost the same chromatogram as shown in Fig. 3. However, it should be noted that the enzymatic digestion resulted in inosine instead of adenosine to some extent. The conversion of adenosine to inosine seems to arise from degradation by an adenosine deaminase which may be associated with the enzymes, probably calf spleen phosphodiesterase, as an impurity.

In Fig. 3, five peaks, assigned to the platinum adducts, were identified by coinjection of the digested sample and the independently prepared platinated nucleotides and nucleosides, Pt(*RSS*-dach)(d(GpG))-1, Pt(*RSS*-dach)(d(GpG))-2, Pt(*RSS*-dach)(d(ApG))-1, Pt(*RSS*-dach)(d(ApG))-2, and Pt(*RSS*-dach)(dG)₂. Unidentified products, marked with asterisks, accounted for approximately 8% of all the products. The reference compounds,

Pt(*RSS*-dach)(d(GpG))-1 and Pt(*RSS*-dach)(d(GpG))-2, were prepared by the reaction of Pt(*RSS*-dach)Cl₂ with d(GpG) and purified by HPLC. They were confirmed to be Pt(*RSS*-dach)(d(GpG)-N7,N7), on the basis of their UV spectral pattern and the p*K*_a value of the N1 of the guanine residue.^{7a,8)} The detailed structures are shown later. The Pt(*RSS*-dach)(d(ApG))-1 and Pt(*RSS*-dach)(d(ApG))-2 were also confirmed to be Pt(*RSS*-dach)(d(ApG)-N7,N7) in the same way.^{4d,9)} The Pt(*RSS*-dach)(dG)₂ was prepared by reaction of 2'-deoxyguanosine with Pt(*RSS*-dach)Cl₂ and confirmed to be Pt(*RSS*-dach)(dG-N7)₂.

It is clear that Pt(*RSS*-dach)Cl₂ reacts preferentially with adjacent purine residues on the DNA, especially the -GpG- and -ApG- sequences. Figure 4 shows a plot of the peak areas of the five products vs. *r* (*r*=amount of Pt(*RSS*-dach)Cl₂ added/amount of base). Binding of Pt(*RSS*-dach)Cl₂ to the -GpG- sequence on the DNA is most marked. The relative peak area of Pt(*RSS*-dach)(d(GpG)) accounts for 67.5–72.0% of all the platinum adducts and tends to increase slightly with decreasing *r*. The nearest-neighbor frequency of the -GpG- sequence in calf thymus DNA (GC content 42%) is calculated as 4.4% and that of the -ApG- sequence as about 6.1%. That is, the statistical probability of the -GG- sequence is lower than that of the -AG- sequence. Experimental results indicate that the peak area of Pt(*RSS*-dach)(d(ApG)) accounts for 13–18% of all the platinum adducts. It can therefore be concluded that formation of Pt(*RSS*-dach)(d(GpG)) is favoured by a factor of 5 over that of Pt(*RSS*-dach)(d(ApG)). The same tendency has also been reported for the reaction products of *cis*-Pt(NH₃)₂Cl₂ with DNA.^{1,3)} In order to elucidate the relative reactivity of Pt(*RSS*-dach)Cl₂ towards the -GpG- and -ApG- sequences, a single stranded oligonucleotide d(TpTpTpGpGpTpTpApGpTpT) was allowed to react with stoichiometric amounts of Pt(*RSS*-dach)Cl₂, and the reaction products were quantified by HPLC after digestion by P1 nuclease and alkaline phosphatase. The reaction gave four products, two of them were Pt(*RSS*-dach)(d(GpG)) and the residual two were Pt(*RSS*-dach)(d(ApG)). It was found that formation of Pt(*RSS*-dach)(d(GpG)) was favoured by a factor of 10 over that of Pt(*RSS*-dach)(d(ApG)). It is therefore unlikely that a duplex structure is required for the strong preference of Pt(*RSS*-dach)Cl₂ for the -GpG- sequence. Such a strong preference for the -GpG- sequence has been also shown in the reaction of *cis*-Pt(NH₃)₂Cl₂ with dinucleotides such as GpG, ApG, CpG, GpA and GpC.¹⁰⁾ Chottard *et al.* indicated on the basis of molecular mechanical calculations that the preference is not only induced by the intrinsically stronger basicity of the N7 site of guanine residue, but it is also enhanced by a hydrogen bonding interaction between the O6 atom of guanine and cisplatin.¹⁰⁾ The Pt(*RSS*-dach)(dG)₂ would arise from both the interstrand crosslinks and intrastrand crosslinks of the two guanines separated by one or more nucleosides, (-Gp(Xp)_nG-).³⁾ The peak area of Pt(*RSS*-dach)(dG)₂ accounts for 6–10% of all the platinum adducts.

Since Pt(*RSS*-dach)Cl₂ lacks a C₂ symmetry element, two geometrical isomers should be formed when platina-

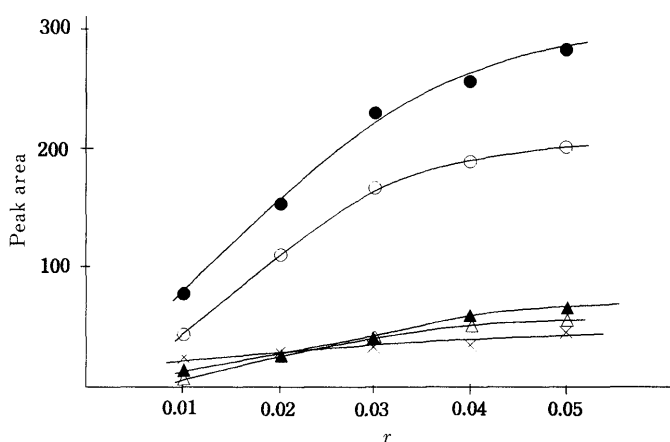


Fig. 4. Variation in Peak Area of the Platinum Adducts Obtained from Pt(*RSS*-dach)-Modified DNA as a Function of *r*

●, Pt(*RSS*-dach)(d(GpG))-1; ○, Pt(*RSS*-dach)(d(GpG))-2; ▲, Pt(*RSS*-dach)(d(ApG))-1; △, Pt(*RSS*-dach)(d(ApG))-2; ◻, Pt(*RSS*-dach)(dG)₂.

$$r = \frac{\text{amount of Pt(RSS-dach)Cl}_2 \text{ added}}{\text{amount of base}}$$

tion occurs at the -GpG- and -ApG- sites. The relative ratio of the geometrical isomers would be interesting. In the reaction of Pt(*RSS*-dach)Cl₂ with d(TpTpTpGpGpTpTpApGpTpT), the ratio of the two geometrical isomers involving d(GpG) was 1:1. The reaction of Pt(*RSS*-dach)Cl₂ with the dinucleotide d(GpG) also revealed an equal amount of the two isomers, *i.e.*, the ratio was 1:1. However, in case of the reaction with DNA, the ratio was 3:2 (see Fig. 4). The ratio remained constant, regardless of the change in *r*.

Reaction Products of Pt(*RSS*-dach)Cl₂ with *r*(GpG) and d(GpG) As mentioned above, Pt(*RSS*-dach)(d(GpG)) was a major product of the reaction between Pt(*RSS*-dach)Cl₂ and DNA, and it consisted of two geometrical isomers. This is theoretically expected because Pt(*RSS*-dach)Cl₂ does not possess a C₂ symmetry element. In order to make clear the distinction between the two isomers, we have synthesized Pt(*RSS*-dach)(d(GpG)) by reacting Pt(*RSS*-dach)Cl₂ with d(GpG) and characterized their structures by NMR spectroscopy. Pt(*RSS*-dach)(*r*(GpG)) was also prepared and used in this work for convenience. Needless to say, the reaction of Pt(*RSS*-dach)Cl₂ with *r*(GpG) resulted in two forms of Pt(*RSS*-dach)(*r*(GpG)). They were separated by preparative HPLC and denoted Pt(*RSS*-dach)(*r*(GpG))-1 and Pt(*RSS*-dach)(*r*(GpG))-2, according to their elution order.

Each isomer of Pt(*RSS*-dach)(d(GpG)) and Pt(*RSS*-dach)(*r*(GpG)) was characterized by ¹H-NMR and pH-titration. Relative integration of the H8 protons of the guanine residues with the methyl protons of the cyclohexane moiety showed that each isomer has the composition Pt(*RSS*-dach)(GpG). From the pH titration of the each isomer, the p*K*_a value at the N1 of the guanine residue was found to be about 8.5, and no protonation was observed on the N7 of the guanine residue. All these observations confirm that each isomer is Pt(*RSS*-dach)(GpG-N7,N7). It is concluded that Pt(*RSS*-dach)(d(GpG))-1 (Pt(*RSS*-dach)(*r*(GpG))-1) and Pt(*RSS*-dach)(d(GpG))-2 (Pt(*RSS*-dach)(*r*(GpG))-2) are geometrical

isomers of each other, as illustrated in Fig. 2.

Conformation of the Cyclohexane and the Chelate Rings

Figure 5 shows the resonances over the range 4.2–0.8 ppm in the NMR spectra of Pt(*RSS-dach*)(d(GpG))-1 and Pt(*RSS-dach*)(d(GpG))-2. Tables I and II indicate the chemical shifts of the cyclohexane and furanose ring protons. Evidently, the axial and equatorial protons of the cyclohexane ring have different chemical shifts, indicating that the rate of inversion of the cyclohexane ring should be slow on an NMR time-scale. This behavior is also true for Pt(*RSS-dach*)(*r*(GpG)) and [Pt(*RSS-*

dach)(NH₃)₂]²⁺. Therefore, it appears that the slow inversion of the cyclohexane ring is due to the methyl inversion at position 3. On the other hand, in the case of Pt(1*R,2S*-cyclohexanediamine)(d(GpG)), which lacks the methyl group, time-averaged signals of the axial and equatorial protons were observed because of a rapid and simultaneous inversion of the cyclohexane and chelate rings.¹¹⁾ From these results, the chelate ring of Pt(*RSS-dach*)(d(GpG)) would adopt either a δ -conformation or λ -conformation as illustrated in Fig. 6.

TABLE I. Chemical Shifts (ppm) of the Cyclohexane Ring Protons of Pt(*RSS-dach*)(LL)

	L = NH ₃	LL = <i>r</i> (GpG)-1	LL = <i>r</i> (GpG)-2	LL = <i>d</i> (GpG)-1	LL = <i>d</i> (GpG)-2
-CH ₃	0.95	0.94	0.96	0.89	0.87
H ¹ _{ax}	2.99	3.05	3.06	2.97	2.99
H ² _{eq}	3.06	3.21	3.35	3.24	3.18
H ³ _{ax}	2.01	2.08	2.07	2.00	1.99
H ⁴ _{ax}	1.11	1.20	1.19	1.07	1.08
H ⁴ _{eq}	1.50	1.60	1.55	1.48	1.48
H ⁵ _{ax}	1.33	1.40	1.36	1.30	1.32
H ⁵ _{eq}	(1.81)	(1.93)	(1.88)	1.80	1.84
H ⁶ _{ax}	1.71	2.24	(1.88)	1.92	2.07
H ⁶ _{eq}	(1.82)	(1.93)	(1.88)	1.82	1.90

Chemical shifts in parenthesis may have an uncertainty of ± 0.02 ppm because of severe overlap among the signals.

TABLE II. Chemical Shifts of the Furanose Ring Protons of Pt(*RSS-dach*)(LL)

	LL = <i>r</i> (GpG)-1	LL = <i>r</i> (GpG)-2	LL = <i>d</i> (GpG)-1	LL = <i>d</i> (GpG)-2
5'G-H1'	6.08	6.06	6.15	6.17
5'G-H2'	4.41	4.63	2.61	2.56
5'G-H2''	—	—	2.68	2.67
5'G-H3'	4.59	4.50	(4.6)	(4.6)
5'G-H4'	4.37	4.33	4.00	4.03
5'G-H5'	4.14	4.03	3.67	3.82
5'G-H5''	3.92	3.78	3.41	3.62
3'G-H1'	5.90	5.89	6.14	6.14
3'G-H2'	4.53	4.63	2.69	2.67
3'G-H2''	—	—	2.53	2.46
3'G-H3'	4.43	4.48	(4.6)	(4.6)
3'G-H4'	4.30	4.33	4.17	4.11
3'G-H5'	4.11	4.09	4.00	3.99
3'G-H5''	4.00	4.02	4.00	3.99

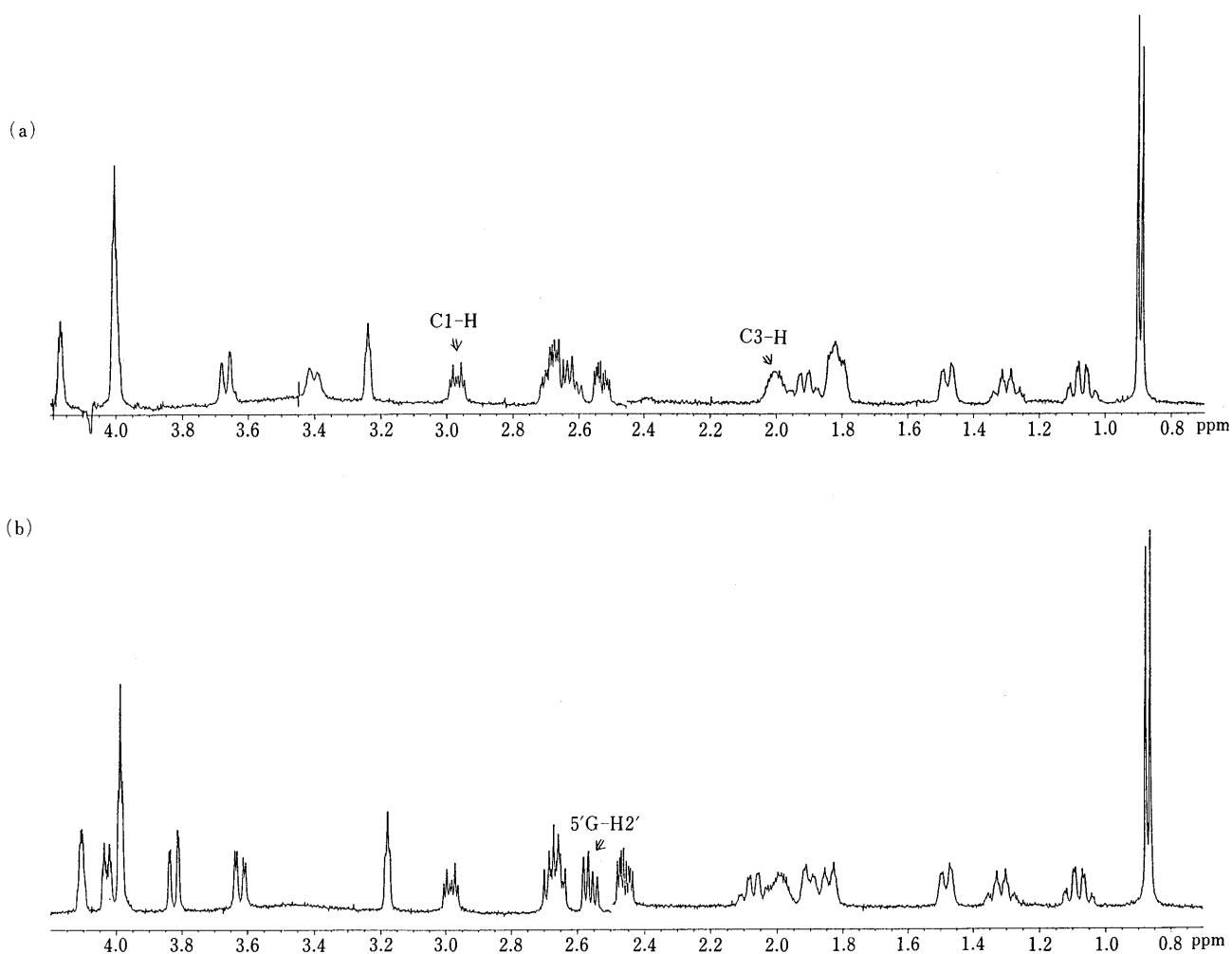


Fig. 5. 500 MHz-NMR Spectra of Pt(*RSS-dach*)(d(GpG))-1 (a) and Pt(*RSS-dach*)(d(GpG))-2 (b)

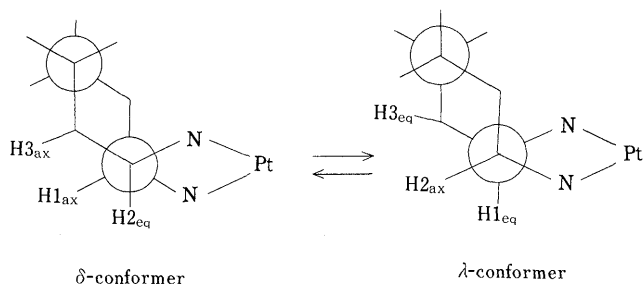


Fig. 6. Possible Conformation of the Cyclohexane and Chelate Rings of Pt(RSS-dach)(GpG)

As shown in Fig. 5, the signals of C1-H (*ca.* 3 ppm) consisted of two triplets, as expected from the vicinal coupling (${}^3J_{1ax-6ax}$, ${}^3J_{1ax-6eq}$ and ${}^3J_{1ax-2eq}$). This means that the C1-H is situated in the axial position and the chelate ring preferentially adopts a δ -conformation. The signals of the C1-H, in the case of λ -conformation should give a quartet, but this was not observed. Molecular modelling also confirms that the δ - is more stable than the λ -conformation. In the δ -conformation, both the methyl group at position 3 and the amino group at position 1 allow the equatorial position to be adopted. The resolution enhancement spectrum shows that the resonance of the C3-H consists of 16 signals. Spectral simulation by the LAOCOON-type microcomputer program supports the conclusion that the C3-H is in the axial position, *i.e.*, the methyl group is in the equatorial position. All the spectral data support the chelate ring having the δ -conformation. Saito and Kidani have also reported that the chelate ring of Pt(RSS-dach)(NH₃)₂ adopted the δ -conformation on the basis of the ${}^3J_{Pt-C3}$ ($=37.8$ Hz) value of the ¹³C-NMR spectrum.⁵⁾ From these results, we can say that the conformation of the chelate ring is actually unaffected by the coordinated d(GpG). The splitting pattern of all the axial and equatorial protons supports the hypothesis that the cyclohexane ring has a chair-type conformation, *e.g.*, the C4-H_{ax} signals agrees well with those (four doublets) expected from ${}^3J_{4ax-3ax}$, ${}^3J_{4ax-5ax}$, ${}^2J_{4ax-4eq}$ and ${}^3J_{4ax-5eq}$. From these results, it is concluded that the cyclohexane and chelate rings of Pt(RSS-dach)(d(GpG)) take the chair and δ -conformation, respectively as illustrated in Fig. 1.

Orientation of the Sugar Moiety of the Guanine Residues

Figure 7 (b and c) shows the resonances over the range 5.8–8.7 ppm for the NMR spectra of Pt(RSS-dach)(*r*(GpG))-1 and Pt(RSS-dach)(*r*(GpG))-2. An assignment of these resonances was carried out with an aid of the two dimensional correlation spectroscopy (2D-COSY) spectrum. A singlet observed at 6.06 ppm for Pt(RSS-dach)(*r*(GpG))-2 was unambiguously assigned to the 5'-G-H1' by following the cross-peaks among the ribose protons of the COSY spectrum. The conformation of the furanose ring is generally represented by a rapid pseudorotational equilibrium between the S-type (C2'-*endo*) and N-type (C3'-*endo*) conformers.¹²⁾ The H1' proton of the 5'-sugar exhibits a sharp singlet which means that the dihedral angle of H1'-C1'-C2'-H2' is almost 90°, *i.e.*, the 5'-sugar has a pure N-type conformer. However the H1' of the 3'-sugar shows a doublet with a coupling

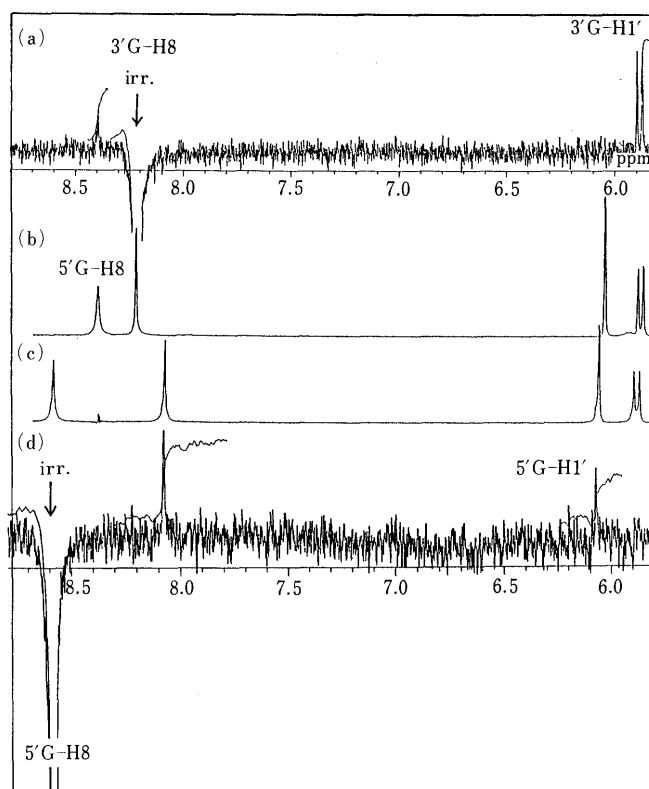


Fig. 7. NOE Difference Spectra of Pt(RSS-dach)(*r*(GpG))-1 (a, b) and Pt(RSS-dach)(*r*(GpG))-2 (c, d)

constant of 6.8 Hz ($={}^3J_{H1'-H2'}$) indicating a predominantly S-type conformation.¹²⁾ In the case of Pt(RSS-dach)(d(GpG)), the resonance of the 5'-G-H1' severely overlapped that of the 3'-G-H1'. Whether the 5'-sugar has an N-type conformer can be obtained from the splitting pattern of the 5'-G-H2' resonance. The 5'-G-H2' signal (2.61 ppm for Pt(RSS-dach)(d(GpG))-1 and 2.56 ppm for Pt(RSS-dach)(d(GpG))-2) indicates a quartet, as shown in Fig. 2, coming from ${}^2J_{H2'-H2''} = -13.3$ Hz, ${}^3J_{H2'-H3'} = 7.5$ Hz and ${}^3J_{H2'-H1'} < 1.0$ Hz. This means that the 5'-sugar adopts the N-type conformation. However the ${}^3J_{H2'-H1'}$ of the 3'-sugar was 7.7 Hz, indicating a predominantly S-type conformation. Such conformational features of the furanose rings have been commonly observed for 17 membered chelate compounds such as *cis*-Pt(LL')(GpG-N7,N7).^{4,9,11)} It is also likely that there is no significant difference in sugar conformation between Pt(RSS-dach)(*r*(GpG)) and Pt(RSS-dach)(d(GpG)).

As is obvious from Fig. 7a, irradiation of the signal at 8.22 ppm (3'-G-H8) resulted in an NOE enhancement for the 3'-G-H1' (5.4%). This indicates that the resonance at 8.22 ppm should be assigned to the 3'-G-H8. Similarly, irradiation of the signal at 8.59 ppm (Fig. 7d) resulted in an NOE enhancement for the 5'-G-H1' (2.5%). In both platinated adducts, the relative orientation of the two guanines is head-to-head because NOE enhancement was observed for the signals between the 5'-G-H8 and 3'-G-H8. Since irradiation at 8.22 ppm (3'-G-H8) also resulted in an NOE enhancement for the 3'-G-H2' (4.63 ppm), the configuration of the guanine base is *anti-anti* towards the 3'-sugar.

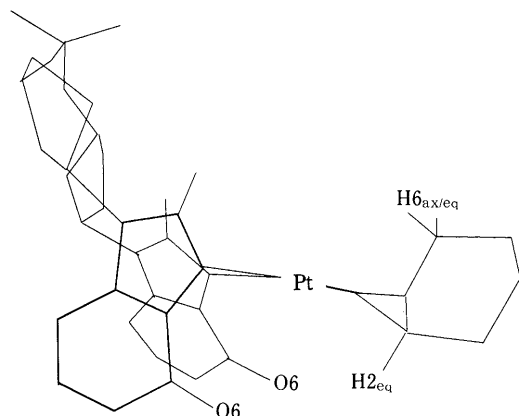


Fig. 8. Proposed Structure of Pt(*RSS-dach*)(*d(GpG)*)-2

Configuration of the Two Geometrical Isomers Table I indicates the chemical shifts of the cyclohexane ring protons of Pt(*RSS-dach*)(*GpG*). In Pt(*RSS-dach*)-(*r(GpG)*), the C2-H_{eq} proton of Pt(*RSS-dach*)-(*r(GpG)*)-2 resonated at a field 0.14 ppm lower compared with that of Pt(*RSS-dach*)-(*r(GpG)*)-1 (Pt(*RSS-dach*)-(*GpG*)-1 is the more rapidly eluting isomer in HPLC). The C6-H_{ax} proton of Pt(*RSS-dach*)-(*r(GpG)*)-1 also resonated at a field 0.36 ppm lower compared with that of Pt(*RSS-dach*)-(*r(GpG)*)-2. The difference in the chemical shifts of the other cyclohexane ring protons was less than 0.05 ppm. One of the molecular models of the two geometrical isomers is depicted in Fig. 8. In such a configuration, the C2-H_{eq} proton faces the O6 side of the guanines, and the C2-H_{eq} proton would experience an anisotropic effect due to the carbonyl group at position 6 of the guanines. This is expected to result in a downfield shift of the C2-H_{eq}. Such behavior is actually observed for the C2-H_{eq} of Pt(*RSS-dach*)-(*r(GpG)*)-2 and Pt(*RSS-dach*)-(*d(GpG)*)-1. It is therefore concluded that Pt(*RSS-dach*)-(*d(GpG)*)-1 has the structure illustrated in Fig. 8. The structure of Pt(*RSS-dach*)-(*r(GpG)*)-2 looks virtually the same as that of Pt(*RSS-dach*)-(*d(GpG)*)-1. In the alternate configuration of the cyclohexane ring, the C6-H_{ax} proton faces the O6 side of the guanines. In such a case, the C6-H_{ax} should experience an anisotropic effect due to the carbonyl group of the guanine residues. This is actually observed for the C6-H_{ax} proton of Pt(*RSS-dach*)-(*r(GpG)*)-1 and Pt(*RSS-dach*)-(*d(GpG)*)-2. Moreover, in a comparison of the molecular models of Pt(*RSS-dach*)-(*GpG*)-1 and Pt(*RSS-dach*)-(*GpG*)-2, the C6-H_{ax} proton is much closer to the O6 compared with the C2-H_{eq}. The C6-H_{ax} proton would therefore experience a stronger anisotropic effect. This is supported by the fact that the difference in the chemical shift of the C6-H_{ax} is larger than that for the C2-H_{eq}.

It is generally found that axial protons resonate at a higher field than do equatorial protons in six-membered cyclohexane derivatives.¹³ That is the case for the cyclohexane ring protons of Pt(*RSS-dach*)(*NH₃*)₂ although the difference in chemical shifts between the C6-H_{ax} and C6-H_{eq} protons is small. It should be noted that the C6-H_{ax} proton is sitting on the square planar coordination plane involving the platinum atom (in the case of the δ -conformation of the chelate ring). The

interaction between the C6-H_{ax} proton and the *d*-electron of the Pt atom moves the C6-H_{ax} to a lower field. The abnormally lower chemical shift observed for the C6-H_{ax} proton can be explained by considering the effect of the *d*-electron in addition to the anisotropic effect of the carbonyl group of the guanines.

As is obvious from Fig. 4, in the case of the reaction with DNA, there is greater formation of Pt(*RSS-dach*)-(*d(GpG)*)-1 than of Pt(*RSS-dach*)-(*d(GpG)*)-2. The most likely interpretation of this is that steric selection may arise from the structural constraints of the DNA double helix. Moreover, it should be noted that Pt(*RSS-dach*)-(*d(GpG)*)-2 has a sterically more crowded structure compared with Pt(*RSS-dach*)-(*d(GpG)*)-1. The reaction between Pt(*RSS-dach*)Cl₂ and the single stranded oligonucleotide resulted in the same amount of the two *d(GpG)* isomers and this may be attributed to the flexibility of the oligonucleotide.

Acknowledgment We thank the Ministry of Education, Science and Culture for financial support for a part of the research under the Grant-in-Aid No. 05640637. We want also to thank Dr. Yukihiisa Kurono and Professor Tamotsu Yashiro of Nagoya City University for their assistance with the NMR experiments.

References and Notes

- 1) a) S. E. Sherman, S. J. Lippard, *Chem. Rev.*, **87**, 1153 (1987); b) J. Reedijk, *Pure. Appl. Chem.*, **59**, 181 (1987); c) W. I. Sundquist, S. J. Lippard, *Coor. Chem. Rev.*, **100**, 293 (1990) and references cited therein.
- 2) a) K. M. Comess, J. N. Burstyn, J. M. Essigmann, S. J. Lippard, *Biochemistry*, **31**, 3975 (1992); b) B. A. Donahue, S. F. Bellon, A. J. Lippard, J. M. Essigmann, "Platinum and Other Metal Coordination Compounds in Cancer Chemotherapy," ed. by S. B. Howell, Plenum Press, New York, 1991, pp. 241–251 and references cited therein.
- 3) a) A. M. J. Fichinger-Schepman, J. L. van der Veer, J. H. J. den Hartog, P. H. M. Lohman, J. Reedijk, *Biochemistry*, **24**, 707 (1985); b) A. Eastman, *Pharmacol. Ther.*, **34**, 155 (1987); c) A. Schwartz, L. Marrot, M. Leng, *ibid.*, **28**, 7975 (1989); d) A. Eastman, *ibid.*, **25**, 3912 (1986).
- 4) a) K. Inagaki, H. Nakahara, M. Alink, J. Reedijk, *J. Chem. Soc., Dalton Trans.*, **1991**, 1337; b) M. J. Bloemink, R. J. Heetebrj, K. Inagaki, Y. Kidani, J. Reedijk, *Inorg. Chem.*, **31**, 4656 (1992); c) J. F. Hartwig, S. J. Lippard, *J. Am. Chem. Soc.*, **114**, 5646 (1992); d) M. Alink, H. Nakahara, T. Hirano, K. Inagaki, M. Nakanishi, Y. Kidani, J. Reedijk, *Inorg. Chem.*, **30**, 1236 (1991).
- 5) R. Saito, Y. Kidani, *Bull. Chem. Soc. Jpn.*, **57**, 3430 (1984).
- 6) K. Satake, Kagaku 1984, appendix (Hardware, NEC PC-9801; Language, N88-Basic).
- 7) a) K. Inagaki, C. Ninomiya, Y. Kidani, *Chem. Lett.*, **1986**, 233; b) B. van Hemelryck, E. Guittet, G. Chottard, J.-P. Girault, F. Herman, T. Huynh-Dinh, J.-Y. Lallemand, G. Igolen, J. C. Chottard, *Biochem. Biophys. Res. Commun.*, **138**, 758 (1986); c) K. Inagaki, Y. Kidani, *Inorg. Chim. Acta*, **106**, 187 (1985); d) K. Inagaki, K. Kasuya, Y. Kidani, *ibid.*, **91**, L13 (1984); e) K. Inagaki, K. Kasuya, Y. Kidani, *Chem. Lett.*, **1983**, 1345.
- 8) K. Inagaki, Y. Kidani, *Chem. Pharm. Bull.*, **33**, 5539 (1985).
- 9) a) K. Inagaki, M. Alink, A. Nagai, Y. Kidani, J. Reedijk, *Inorg. Chem.*, **29**, 2183 (1990); b) K. Inagaki, A. Tomita, Y. Kidani, *Bull. Chem. Soc. Jpn.*, **61**, 2825 (1988).
- 10) A. Laoui, J. Kozelka, J. C. Chottard, *Inorg. Chem.*, **27**, 2751 (1988).
- 11) a) K. Inagaki, Y. H. Nakahara, M. Alink, Y. Kidani, *Inorg. Chem.*, **29**, 4496 (1990); b) K. Inagaki, Y. Kidani, *ibid.*, **25**, 1 (1986); c) M. J. Bloemink, J. P. Dorenbos, R. J. Heetebrj, B. K. Keppler, J. Reedijk, H. Zahn, *ibid.*, **33**, 1127 (1994).
- 12) L. B. Rinkel, C. Altona, *J. Biomol. Struct. Dyn.*, **4**, 621 (1987).
- 13) A. Gaudemer, "Stereochemistry," ed. by H. B. Kagan, Georg. Thieme Publishers, Stuttgart, 1977, pp. 44–136.